Published in final edited form as:
Stem Cells. 2013 August ; 31(8): 1548–1562. doi:10.1002/stem.1415.

Improved cell therapy protocol for Parkinson's disease based on differentiation efficiency and safety of hESC-, hiPSC and non-human primate iPSC-derived DA neurons

Sundberg Maria[1], **Bogetofte Helle**[1,#], **Lawson Tristan**[1,2], **Smith Gaynor**[1], **Astradsson Arnar**[1], **Moore Michele**[1,2], **Osborn Teresia**[1], **Cooper Oliver**[1], **Spealman Roger**[2], **Hallett Penelope**[1], and **Isacson Ole**[1,*]

[1]Neuroregeneration Laboratories, Harvard Medical School/McLean Hospital, Belmont, MA, 02478

[2]New England Primate Research Center, Harvard Medical School, Southborough, MA 01772

Abstract

The main motor symptoms of Parkinson's disease are due to the loss of dopaminergic (DA) neurons in the ventral midbrain (VM). For the future treatment of Parkinson's disease with cell transplantation it is important to develop efficient differentiation methods for production of human iPSCs and hESCs-derived midbrain-type DA neurons. Here we describe an efficient differentiation and sorting strategy for DA-neurons from both human ES/iPS cells and non-human primate iPSCs. The use of non-human primate iPSCs for neuronal differentiation and autologous transplantation is important for pre-clinical evaluation of safety and efficacy of stem cell-derived DA neurons. The aim of this study was to improve the safety of human- and non-human primate-iPSC (PiPSC)-derived DA neurons. According to our results, $NCAM^{+}/CD29^{low}$ sorting enriched VM DA-neurons from pluripotent stem cell-derived neural cell populations. $NCAM^{+}/CD29^{low}$ DA-neurons were positive for FOXA2/TH and EN1/TH and this cell population had increased expression levels of *FOXA2*, *LMX1A*, *TH*, *GIRK2*, *PITX3*, *EN1*, *NURR1* mRNA compared to unsorted neural cell populations. PiPSC-derived $NCAM^{+}/CD29^{low}$ DA-neurons were able to restore motor function of 6-OHDA lesioned rats 16 weeks after transplantation. The transplanted sorted cells also integrated in the rodent brain tissue, with robust TH+/hNCAM+ neuritic innervation of the host striatum. One year after autologous transplantation, the primate iPSC-derived neural cells survived in the striatum of one primate without any immunosuppression. These neural cell grafts contained FOXA2/TH-positive neurons in the graft site. This is an

*Corresponding author: isacson@hms.harvard.edu.
#Current address: The Institute of Molecular Medicine, University of Southern Denmark, Odense, Denmark

Author contributions:
M.S.: planning of experiments, cell culture and differentiation, cell sorting experiments, in vivo procedures, data analysis, writing of manuscript
H.T.: cell culture and differentiation, discussion of data and experiments
T.L.: cell culture and differentiation, discussion of data and experiments
G.S.: in vivo procedures, discussion of data and experiments
A.A.: in vivo procedures, discussion of data and experiments
M.M: in vivo procedures, behavioral analyses, discussion of data and experiments
T.O.: in vivo procedures, discussion of data and experiments
O.C.: planning of experiments, data analysis, discussion of data and experiments
R.S.: planning of experiments, data analysis, discussion of data and experiments
P.H.: planning of experiments, in vivo procedures, data analysis, discussion of data and experiments
O.I.: planning of experiments, data analysis, discussion of data and experiments, writing of manuscript

Disclosure of Potential Conflicts of Interest
The authors indicate no potential conflicts of interest.

important proof of concept for the feasibility and safety of iPSC-derived cell transplantation therapies in the future.

Introduction

Parkinson's disease (PD) is a chronic and progressive movement disorder, mainly caused by death of dopaminergic (DA) neurons in the ventral mesencephalon (VM). It has been shown that cell replacement therapy with fetal VM DA neurons can be beneficial for PD patients [1, 2]. Since there is very restricted availability of fetal tissue, human embryonic stem cells are considered to be an optional source for derivation of specialized DA neurons for the future cell therapy of PD [3–5]. VM DA neurons arise from floor plate cells during embryonic development [6]. It has previously been described that sonic hedgehog (SHH), fibroblast growth factor 8a (FGF8a) and Wnt1 are important and sufficient for differentiation of VM DA neurons [7–10]. For generation of human pluripotent stem cell derived- DA neurons, recently published protocols are mimicking embryonic development in a dish by activating transcription factor pathways important for VM DA neuron derivation [3–5]. Based on these studies, efficient floor-plate induction with highly activated SHH and neural induction with dual SMAD-inhibition induces derivation of VM floor plate cells with neurogenic potential in human pluripotent stem cell cultures [3–5]. These studies also show that inhibition of GSK-3β in the wnt-signalling pathway drives efficient differentiation of VM DA neurons [3–5]. Although these methods are quite usable, in order to ensure an appropriate DA neuron patterning, signaling parameters for cell lineage specification must be further optimized and identified.

Pluripotent stem cell-derived cell populations pose a risk for tumor formation after transplantation, since the cell populations can contain undifferentiated cells or proliferating non-neural cells [11–13]. In order to solve this issue, several sorting methods have been developed for enrichment of differentiated neural cell populations and eliminating pluripotent stem cells using FACS or MACS. Heterogeneous pluripotent stem cell -derived neural cell populations can be purified using different combinations of CD-markers [14–16] or sorting of transgenic ES cell lines during DA neuron differentiation; Hes::GFP, Nurr1::GFP, Pitx3::GFP [17, 18]. Anti-Corin antibody has been tested for enrichment of VM neurons from differentiated ES cells [6]. However, sorting of fluorescence tagged DA neuron precursor cells requires gene manipulation, which is not preferable for clinical settings. Also, scalability of corin- sorting is limited due to the low expression level and limited developmental time window for protein expression [6]. Currently there are no single markers that could be used safely and efficiently to eliminate pluripotent stem cells, distinguish non-neurogenic floor plate precursors from VM floor plate precursors, and enrich specialized DA neurons from pluripotent stem cell-derived neural populations.

The aim of our study was to develop and optimize an efficient differentiation and sorting method for purification of specialized DA neurons from pluripotent stem cells. We developed this method using pluripotent stem cells derived from different sources: human embryonic stem cells (hESC), human induced pluripotent stem cells (hiPSC) and non-human primate induced pluripotent stem cells (PiPSC). Our aim was also to characterize subpopulations of differentiating DA neurons and study the safety and functionality of unsorted and sorted pluripotent stem cell-derived DA neuron populations in PD-animal models.

Materials and Methods

Culturing of pluripotent stem cells

Pluripotent stem cell lines used in this study: human ESC line H9 (National Institute Health code WA09; Wisconsin Alumni Research foundation, Madison, WI), human iPSC lines: 2135 and 1815 (derived from adult skin fibroblasts, characterized in [19]), and non-human primate iPSC lines: MF95.06, MF27.04, MF66.02 and MF25.04 (derived from cynomolgus macaque skin fibroblasts, characterized previously in [20]). Pluripotent stem cell colonies were maintained on irradiated mouse embryonic fibroblasts (MEF CF-1 IRR, Global Stem®) in ES-medium. ES-medium consists of: DMEM/F12 (Gibco, Life Technologies, USA), 20 % Knock-Out serum replacement (Gibco, Life Technologies), 1 % MEM-NEAA (Gibco, Life Technologies), 1X l-glutamine (Gibco, Life Technologies), penicillin 100 units/ml, streptomycin 100 μg/ml (Gibco, Life Technologies), 1X β-mercaptoethanol, bFGF 8 ng/ml. Cell colonies were passaged every 6–9 days by manual picking and re-plated to fresh MEFs (MEF density 185,000cells/well in a 6-well plate). For upscaling the cell cultures, the stem cell colonies were passaged with collagenase IV-treatment (5min +37°C, inactivation with ES-medium) and cell clusters were re-plated to fresh MEFs or GF-reduced Matrigel (BD Biosciences, USA) in mTESR1 (Stem Cell Technologies, USA) with ROCK-inhibitor (Y-27632, Sigma, USA) 10 μM.

Differentiation of DA neurons from pluripotent stem cells

In all differentiation experiments stem cell colonies were either manually picked or enzymatically split to single cells and re-plated to GF-reduced Matrigel (BD Biosciences) in mTESR1 (Stem Cell Technologies) or conditioned ES-medium supplemented with ROCK-inhibitor (Y-27632, Sigma) 10 μM and bFGF 10 ng/ml (Invitrogen, Life Technologies). The differentiation protocol for Method A was modified according to Kriks et al. 2011 [4, 21]. In differentiation Methods B-D different combinations of small molecules were tested for floor plate induction and neural differentiation: SB431542 10 μM (SB, Sigma), LDN-193189 100 nm (LDN, Stemgent, USA), SAG 1 μM (Enzo, Life Sciences, USA). In Methods B-D GSK-3β inhibitor CHIR99021 (CHIR, Stemgent) was tested with three different concentrations: 0, 1, and 3 μM at different time points (0–13 days or 3–13 days). During differentiation (0–13 days) Methods B-D also included: +/−Noggin 600 ng/ml (R&D Systems, USA), FGF8a 100 ng/ml (R&D Systems, USA), wnt-1 100 ng/ml (Peprotech Inc., USA), retinoic acid 10^−8 M (Sigma). Cells were passaged with Accutase (StemPro®, Gibco, Life Technologies) after 20 days of differentiation and re-plated to poly-l-ornithine 15 %/laminin 2 μg/ml/fibronectin 2 μg/ml coated plates (all from Sigma). See Figure 1 for details of the Methods A–D.

For Methods A-D the following basic mediums were used: SRM (days 0–5): Knock-Out DMEM (Gibco, Life Technologies), 15 % Knock-Out serum replacement (Gibco, Life Technologies), penicillin 100 units/ml, streptomycin 100 μg/ml (Gibco, Life Technologies), 1X β-mercaptoethanol, 1X MEM-NEAA (Gibco, Life Technologies). Sequential addition of N2-medium: 25 %, 50 %, 75 % and 100 % (between days 5–8) and 100 % N2-medium (between days 9–11): DMEM/F12 (Gibco, Life Technologies), 1X N2-supplement (Stem Cell Technologies). The following medium and growth factors were used for the final DA-neuron differentiation (days 11–30, Methods A-D): Neurobasal-medium (Gibco, Life Technologies), 1X B27-supplement (Gibco, Life Technologies), 1X l-glutamine, BDNF 20 ng/ml, GDNF 20 ng/ml (both from Peprotech Inc.), cAMP 0.5 mM (Enzo, Life Sciences), TGF-β3 2ng/ml (Calbiochem, USA), Ascorbic Acid 200 μM (Sigma), γ-secretase inhibitor 10 nM (Millipore, USA).

Sorting of DA neurons with FACSAria

After 30 days of differentiation, iPSC-derived DA neuron populations were treated with 0.05% trypsin-EDTA (Gibco, Life Technologies) for 5 min at 37°C and trypsin was inactivated with 10 % FBS-HBSS-pen/strep. Single cells were stained with NCAM (Eric1, Santa Cruz) for 30 min at RT, washed twice with 10 % FBS-HBSS-pen/strep before addition of anti-mouse IgG Alexa488 (Molecular Probes, Life Technologies) for 30 min in the dark. Cells were co-stained with CD29-APC (BD Biosciences) for 30 min in the dark and washed with 10 %FBS-HBSS-pen/strep. Cells were sorted with FACSAria (BD Biosciences) using settings for sensitive cells as previously described [15, 22]. Briefly, FACSAria was prepared for aseptic sorting with 70 % Ethanol-clean and sterile autoclaved dPBS was used for fluidics sheath. 100 μM nozzle was used for the sorting with sheath pressure 18.00 PSI. Accudrop beads (BD) were used for determining stream stability and CS&T beads (BD) for validation of laser settings. Unstained cells were used for determination of SSC/FSC – parameters. For setting of fluorochrome channels (FITC-A and APC-A) and for elimination of background staining cells were stained with secondary antibodies only: anti-mouse IgG Alexa 488 (Molecular Probes, Life Technologies) or isotype control mouse IgG-APC (BD Biosciences).

Flow cytometry

hESC-, hiPSC- and PiPSC-derived neural cells were stained for surface marker expression profiles after 14 and 30 days of differentiation *in vitro* as previously described [14]. Briefly, neural cell populations were treated with 0.05 % trypsin-EDTA (Gibco, Life Technologies) for 5 min +37°C and trypsin was inactivated with 10 % FBS-HBSS-pen/strep. Approximately 1,000,000 cells were used for each sample. In the case of unconjugated antibodies, cells were incubated with primary antibodies for 30 min at room temperature, after which cells were washed with 10% FBS-HBSS and incubated with fluorescence-tagged secondary antibodies for 20 min. Simultaneously, cells were incubated with ready conjugated antibodies (see Supplemental Tables 1–3) for 20 min, and washed with 10% FBS-HBSS and analyzed with FACSAria. For elimination of background staining, cells were stained with secondary antibodies only or isotype controls. For multicolor stainings, overlapping of fluorochrome channels was eliminated with compensation samples containing individually stained cells for each antibody studied. 30,000 events were recorded for each sample and analysis was repeated at least two separate times for each cell line.

Gene expression analysis

For gene expression analysis, the RNA was isolated from unsorted and sorted cell samples using RNeasy MicroKit (Qiagen, USA) according to manufacturers instructions. 85–150 ng of RNA was used for cDNA preparation using Superscript™III First-Strand Synthesis System for RT-PCR (Invitrogen) according to manufacturers instructions. Quantitative qRT-PCR reaction was performed with ABI Prism (Applied Biosystems, USA) using Power SYBER® Green Master Mix and RTqPCR primers (Qiagen, see Table 4 for details). The expression of the gene of interest was determined in triplicate samples for each cell culture condition. β-actin was used as reference gene. The Ct value of each target gene was normalized against the Ct value of the reference gene (Ct(target)-Ct(β-actin)). Results were analyzed using the ΔΔCt method (ΔCt(sorted sample)-ΔCt(unsorted control)). The relative expression was calculated 2^-ΔΔCt and represented as fold change of gene expression compared to unsorted cell sample (=1). If the values were <1 the decrease in relative gene expression was calculated with the following equation 1/−2^-ΔΔCt. Each analysis was repeated at least twice.

6-OHDA lesioned rats

All animal procedures were performed according to National Institutes of Health guidelines and were approved by the Institutional Animal Care and Use Committee at McLean Hospital and Harvard Medical School. Adult female rats (Sprague-Dawley, 200–250g) with unilateral 6-OHDA lesions [23–25] were purchased from Taconic Farms, (Taconic Farms Inc., Germantown, NY). 6-OHDA lesions were prepared as described by supplier. Briefly, an infusion cannula was stereotaxically placed via a hole in the skull and located within the nigrostriatal pathway, coordinates from bregma: AP:−4.3, ML: 1.2, DV:−8.3. A 2 μg/μl solution of 6-hydroxydopamine was infused at a rate of 1μl/min for 4 minutes. Following drug infusion the skin incision was closed with stainless steel wound clips. To evaluate the lesion, animals were monitored by a two-step evaluation of the response to a subcutaneous injection of apomorphine. The first injection was given 14 days post-lesion (0.2mg/kg), the second injection was given 21 days post-lesion (0.05mg/kg). After drug injections the animals were placed in a rotometer and the rotational behavior contra lateral to the lesion side was recorded quantitatively for 6 consecutive 5-minute periods (30 minutes total). Following the 21-day evaluation, only animals with positive results (total of >180 rotations/30 minutes) were used for transplantation experiments.

Transplantation of iPSC-derived DA neurons to 6-OHDA-lesioned rats

Unsorted PiPSC-derived DA neurons and $NCAM^{+}/CD29^{low}$ sorted PiPSC-derived DA-neurons were suspended to 50, 000 cells/μl-100, 000 cells/μl in HBSS (Gibco, Life Technologies) supplemented with 20mM D-glucose (Sigma) and 1 μg/ml GDNF (Peprotech). 2 μl of cell suspension were transplanted to two deposits of the following coordinates from bregma: Site 1: anteroposterior +0.4, mediolateral −3.0, dorsoventral −5.0. Site 2: anteroposterior −0.5, mediolateral −3.6, dorsoventral −5.0. To prevent graft rejection all animals were immunosupressed with cyclosporine A injections (30 mg/kg, Sandimmune; Sandoz) starting one day before surgery, and continuing with daily injections at 15mg/kg/day (s.c.).

Behavioral tests and transplantation groups of 6-OHDA rats

Two weeks before transplantation rotational asymmetry of 6-OHDA-lesioned rats was analyzed after s.c. injection of apomorphine (0.1 mg/kg; 40min) or i.p. injection of amphetamine (4mg/kg; 90 min). Lesioned rats were randomly divided into different groups according to behavioral responses. Amphetamine- and apomorphine-induced rotations were evaluated 8, 12, and 16 weeks after transplantation. For spontaneous movement tests animals were evaluated with cylinder-test and stepping adjustment test after 16 weeks of transplantation as previously described [26]. The control group consisted of 6-OHDA-lesioned rats without cell graft (n= 9), the cell transplantation groups consisted of: unsorted PiPSC-DA neurons (MF95.06-line, n= 4), unsorted PiPSC-DA neurons (MF25.04-line, n= 6) or sorted $NCAM^{+}/CD29^{low}$ PiPSC-DA neurons (MF25.04, n=8). In parallel with the autologous monkey transplantation, unsorted PiPSC-DA neurons (MF27.04-line and MF66.02-line) were transplanted to 6-OHDA rat striatum (n=6/line) on the same day and using the same cell batch.

PiPSC-derived DA-neurons for autologous transplantation

PiPSCs (MF27.04 line) were differentiated using a feeder-free method modified from Method C with CHIR 1 μM for 0–9 days of differentiation (Figure 1). In order to increase cell amounts for transplantation, an additional proliferation step was added for cells between 11–19 days of differentiation: N2-medium supplemented with BDNF, AA, SAG, FGF8a. Final DA-neuron differentiation was done in the N2-medium supplemented with BDNF, cAMP, TGFb, GDNF, AA (using concentrations described above). For preparation of

PiPSC-derived neuronal cells for transplantation, cells were treated with 0.05% trypsin-EDTA 3min +37 °C. Trypsin was inactivated with 10% FBS-dPBS and cells were centrifuged for 3min at 1000rpm, and re-suspended in HBSS+ 20mM Glucose +GDNF 1μg/ml. Viability of cells was determined with Trypan Blue staining. Cells were centrifuged 3min at 1000rpm and re-suspended at a density of 200,000 cells/μl HBSS+ 20mM D-Glucose +GDNF 1μg/ml. The concentration of VM type DA-neuron cells was approximately 4,000–6,000 FOXA2/TH+ cells/μl.

Autologous transplantation of PiPSC-derived DA neurons to MPTP-treated cynomolgus macaque

Induction of parkinsonism was performed as previously described [27, 28]. In brief, a male cynomolgus monkey received weekly i.v. injections of 1-methyl, 4-phenyl, 1,2,3,6-tetrahydropyridine (MPTP) (0.3 mg/kg per week for 5 weeks, total dosage 8.4 mg) that resulted in mild stable parkinsonism (Parkinsonian Rating Scale [PRS] score = 11 [total score from 0–24]). Global motor activity scores were collected using activity monitors (AW64 Actiwatch, Philips Electronics) [29], worn one week at a time every 2–4 months. Transplantation sites were defined using e-film version 1.8.3 (merge eFilm, Milwaukee, http://www.merge.com) on axial T1 and coronal T2 magnetic resonance images (MRI) coronal MR T2 images of the monkey brain obtained with the animal under general anesthesia placed in the same stereotactic frame used for the surgery. Four sites were defined in the left postcommissural putamen. Surgery was performed in sterile conditions under isoflurane anesthesia with assisted ventilation. After cranial preparation, a skin incision was made over the target area, and skin, muscle, and fascia were retracted to expose the cranial surface. A burr-hole was drilled over the target area, and 25 μl of the cell suspension were slowly (2 μl/minute) injected along a 4 mm tract (19 to 15 mm ventral from the dura) at each antero-posterior site, using a 20 gauge beveled 45° point needle. After completion of all injections, the surgical site was washed, the burrhole sealed with bone wax, and the fascia, muscle, and skin were sutured in planes. Twelve months after the transplant, the animal was sedated with ketamine (15 mg/kg) and anesthetized with pentobarbital (Nembutal; 25 mg/kg, i.v.) and perfused transcardially with ice-cold heparinized saline followed by 4% paraformaldehyde. The brain was postfixed overnight and equilibrated in graded sucrose solutions (10%–30% in PBS) and sectioned on a freezing microtome in 40-μm slices that were serially collected.

Immunohistochemistry

For immunohistochemical analysis, animals were intracardially perfused with heparinized saline solution (0.1 % heparin in 0.9 % saline solution) and 4 % paraformaldehyde (pH 7.4) after i.p. overdose of pentobarbital (150 mg/kg). Perfused brains were cryoprotected in 30 % sucrose and sectioned on a microtome in 40 μm slices. After 1 hour of blocking in 10 % NDS-0.1 % TritonX in dPBS, primary antibodies were added for sections and incubated for 2 days at + 4°C. Secondary antibodies were added after washes with 0.1 % TritonX in dPBS and incubated for 1h at RT. After washes nuclear staining was performed with Hoechst 33342 (5 μg/ml: Life Technologies).

TH, NCAM and HLA staining and cell counting with Stereo investigator

For TH-DAB, hNCAM-DAB and HLA-DAB staining, brain sections (40 μm) were treated with 3 % H_2O_2 for 7min to remove endogeneous peroxidases. Sections were washed with dPBS and blocked using 10 % NDS in PBS for 1 hour at room temperature. Primary antibody rabbit anti-TH (Pel-Freeze, 1:300) or mouse anti-human NCAM (Santa-Cruz, 1:100), or mouse anti-human HLA-DP (clone CR3/43, 1:100, Dako) was added in 10% NDS for over night incubation at room temperature. Secondary antibodies; biotinylated anti-rabbit IgG or biotinylated anti-mouse IgG (1:300, Vector Laboratories) were added to

sections after washes and incubated for 1 hour. Sections were then treated with strepavidin-biotin complex (Vectastin ABC kit Elite: Vector Laboratories) and nickel, and visualized by incubation in 3,3′-diaminobenzidine (Vector Laboratories). Brain sections were mounted and dehydrated with ethanol series: 70% EtOH 3min, 95% EtOH 3min, 100% EtOH 3min, and xylene 5min x2. An Olympus Microscope and the Stereo Investigator software were used for TH+ cell counting and TH+ fiber counts. For evaluation of the total number of cells and volume of the graft every sixth section with graft was counted using cavalieri estimator. For density analysis of TH-staining intensity, every sixth section was imaged with Spot-program (16-bit full resolution tiff-image from the striatum) using constant exposure time and settings, and pictures were inverted with ImageJ for raw intensity density analysis. Number of rats in each group analyzed: unsorted PiPSC-neural grafts n=5, $NCAM^{+}$/$CD29^{low}$ neural grafts n=8, lesion controls n=9.

Immunocytochemistry

For immunostainings, cells were fixed with 4 % paraformaldehyde for 20 min at RT. For blocking of the background staining cells were incubated with 10 % normal donkey serum (NDS)/normal goat serum (NGS) in 0.1% TritonX in dPBS for 1h at RT. Primary antibodies were added for the cells in 10 % NDS/NGS-0.1% TritonX in dPBS for over night staining in +4 °C. After primary staining cells were washed with 0.1% TritonX in dPBS and secondary antibodies were added to the cells in 10 % NDS/NGS-0.1% TritonX in dPBS for 1h RT. Primary and secondary antibodies used are listed in the supplemental Tables 2–3. For nuclear detection cells were stained with hoechst (Invitrogen, Life Technologies) and coverslips were mounted with mowiol (Sigma).

Statistical analysis

Statistical analysis for cell counts was performed with Instat program: Kruskall wallis test (Non-parametric ANOVA) between groups, and Dunn's Multiple Comparisons Test was done between selected pairs of groups. For comparison of statistical differences between two individual groups non-parametric Mann-Whitney test with two-tailed P value was used. P values < 0.05 were considered statistically significant.

Results

Development of DA neuron differentiation protocols for hESCs

Early patterning of DA neuron precursor cells from floor-plate derived cells— To develop an optimal differentiation protocol for VM DA neurons we differentiated hESCs on growth-factor reduced matrigel with different combinations of small molecules; LDN, SB, SAG, purmorphamine, RA, and recombinant proteins; SHH, FGF8a, wnt1, and noggin (schematic presentation of methods A–D in Figure 1A). According to our results, and a previously published protocol [4], Method A in Figure 1, most efficiently supports the early patterning of hESCs and derivation of FOXA2/OTX2–positive ventral midbrain type DA-neuron precursors (DIV9, Figure 1B). Cells that were differentiated according to Method A were positive for floor-plate derived DA neuron precursors markers: FOXA2 (>55 %), OTX2 (>75%), FOXA2/OTX2 (>50%) and FOXA2/OTX2/β-tubulinIII (>30%) at significantly higher levels after 9 days compared to the other conditions ($p<0.05$, Figure 1B). After 9 days of differentiation in the absence of CHIR (0 μM) and presence of recombinant wnt1 (100ng/ml) the number of OTX2+ and FOXA2+/OTX2+ was significantly lower compared to Method A with 3 μM CHIR.

Efficient GSK-3β inhibition is important for floor-plate derived DA neuron differentiation—Next we wanted to compare the effects of timing of floor-plate induction and GSK-3β inhibition for DA-neuron precursor derivation and differentiation from hESCs.

In Methods A and B, SHH, purmorphamine or SAG were added to cells after 1 day of neural induction, and CHIR (3 μM) was added to the cells after 3 days of starting of the differentiation. When this relatively high concentration of GSK3-β inhibitor CHIR (3 μM) was used in Methods C and D in addition to the other factors in the beginning of differentiation, the number of OTX2+ and FOXA2/OTX2+ cells was significantly lower after 9 days of differentiation (Figure 1B, DIV9). In addition to this, with high concentration of CHIR (3 μM) the number of FOXA2+, FOXA2/TH+ cells was significantly lower after 30 days of differentiation in Methods C and D compared to Method A and B (Figure 1C, DIV30). When concentration of GSK-3β-inhibitor was lowered in Methods C and D (CHIR 1 μM) the number of OTX2+ and FOXA2/OTX2+ cells increased (DIV9). In addition to this, derivation of FOXA2/TH+ DA-neurons from hESCs using Methods C-D with CHIR (1 μM) was as efficient as in Method A and B with CHIR (3 μM) (>15–20% from total cell population, DIV30). According to these results we selected method A as the standard condition for the pluripotent stem cell-derived DA neuron differentiation for all the further experiments reported here. Method C with CHIR (1 μM) and an additional cell proliferation step was used for preparation of PiPSC-derived DA neurons for autologous transplantation of cynomolgus macaque (see Materials and Methods). To increase the number of progenitor cells prior to differentiation, the additional proliferation step is important. During differentiation with this method the overall percentage yield did not change significantly compared to method A.

Characterization of hESC-, hiPSC- and PiPSC-derived DA neuron precursors and DA neurons

To characterize DA neurons derived from different cell origins we performed flow cytometric analysis and immunocytochemical cell counting for hESC-, hiPSC- and non-human primate (PiPSC)-derived cells (Figure 2). The expression of pluripotency markers Tra 1–81 and SSEA-4 was downregulated after 30 days of differentiation, to < 0.5 % Tra1–81 and <5 % SSEA-4 in hESC and hiPSC-derived cells. However, the PiPSC-derived cell population included up to 30 % of SSEA-4 positive cells even after 30 days of differentiation (Figure 2B). Expression of the neural precursor markers CD184 (CXCR4) and CD56 (NCAM) was upregulated during floor-plate derived neural cell differentiation in human stem cell lines (Figure A–B). In PiPSC-derived cell populations the expression of CD184 and CD56 was already >40% after 14 days of differentiation and increased up to 50–60% after 30 days of differentiation. Most interestingly the expression of $CD56^{+}/CD29^{low}$ increased in all the studied cell lines from 10% (day 14) up to 35%–40% (day 30). Expression of the neuronal marker CD271 (p75 neurotrophin receptor) increased from <5% to >40% in hESC and hiPSC-derived cells. However, CD271 was not expressed as consistently in PiPSC-derived cells (0% day 14 to >10% at day 30) (Figure 2A–B). Expression of the floor-plate cell marker CD29 (β-integrin) was consistent between 14 to 30 days of differentiation >60% in all the cell lines studied (Figure 2A–B). According to immunocytochemical characterization hESC-, hiPSC-, and PiPSC-derived DA-neurons expressed FOXA2 >50–70%, TH >10–20%, FOXA2/TH >10–20%, β-tubulinIII 30–40%, FOXA2/β-tubulinIII >30–35%, Calbindin 5–10%, FOXA2/TH/Calbindin 5%, Tryptophanhydroxylase/TH-negative <5%, serotonin/TH-negative < 5%. Although PiPSC-derived cells had higher expression levels of neural markers after 14 days of differentiation, there were no statistically significant differences in neural marker expression profiles after 30 days of differentiation (Figure 2A–F).

Characterization of hESC- and hiPSC- derived –neural subpopulations and enrichment of DA neurons with cell sorting

To select optimal markers for enrichment of DA-neurons we characterized gene- and protein expression profiles of hESC- and hiPSC-derived neural subpopulations. According to our

results, the NCAM^{low}–population included a subpopulation of cells that expressed the mesodermal-lineage specific marker KDR (11–16%) and the pluripotency marker SSEA-4 (2–8%) (Figure 3C). The NCAM^{+} population was highly positive for CD29 (β-integrin > 65%). The NCAM^{+} population also included a subpopulation of neuronal cells that were positive for CD24^{+}/CD29^{low} (12–24%) and a subpopulation of neural stem cells that were positive for CD184^{+}/CD133^{low} (24–34%) (Figure 3D). According to the quantitative gene expression analysis, the combinatorial sorting strategy with NCAM^{+}/CD29^{low}–selection resulted in a significantly higher expression of DA neuron specific genes compared to NCAM^{+}, NCAM^{low}, or CD29^{+} selection (Figure 3F). In particular, *NURR1*, *GIRK2*, *PITX3* and *TH* were upregulated in the NCAM^{+}/CD29^{low} cell population compared to unsorted neural cells, NCAM^{low}, and CD29^{+} cells (Figure 3F). According to these results, we chose the NCAM^{+}/CD29^{low} selection method for enrichment of hESC- and hiPSC-derived DA-neurons at day 25–30 of differentiation. After sorting with NCAM^{+}/CD29^{low} selection, the percentage of NCAM-positive and β-tubulinIII-positive cells increased from 60% (before sorting) to >80% (after sorting). Most importantly, the number of TH-positive cells increased significantly after NCAM^{+}/CD29^{low} sorting from 20% (before sorting) to 40–50% (after sorting, $p<0.001$ and $p< 0.01$). NCAM^{+}/CD29^{low} sorting increased the percentage of FOXA2/TH-positive and EN1/TH-positive cells significantly from 10–15% (before sorting) to 40% after sorting ($p<0.01$ and $p< 0.05$, Figure 3G). In addition to this, NCAM^{+} and NCAM^{+}/CD29^{low} sorting significantly decreased the amount of FOXA2/TH/Calbindin-positive cells in hiPSC-derived DA-neuron population compared to the unsorted cell population (5% FOXA2/TH/Cb in the unsorted cell population vs <0.4% FOXA2/TH/Cb in the sorted cell populations, Supplemental Figure 1). In the unsorted pluripotent stem cell derived-neural cell populations expression of pluripotency markers SSEA-4 and Tra-1–60 and coriplexus endothelium marker transthyretin were detected in a few individual cells. However, after NCAM^{+}/CD29^{low} sorting no pluripotent cells or endothelium-type cells were detected in hESC- or hiPSC-derived DA neuron populations (Figure 3, Supplemental Figure 1).

Enrichment of PiPSC-derived DA neurons with NCAM^{+}/CD29^{low} sorting

To study the neural subpopulations of differentiated non-human primate iPSCs we sorted cells with NCAM^{+}, NCAM^{+}/CD29^{low}, and NCAM^{low}. According to quantitative gene expression analysis, the NCAM^{+}/CD29^{low} sorted cell population had significantly higher expression levels of *FOXA2*, *LMX1A*, *TH*, *GIRK2*, *PITX3*, *EN1*, *NURR1* and *NCAM* compared to unsorted cells and NCAM^{low} cells (Figure 4B). Similarly to sorted hESC- and hiPSC-derived neural cell populations (Figure 3), the percentages of NCAM, β-tubulinIII, TH, TH/FOXA2, and TH/EN1 increased significantly after NCAM^{+}/CD29^{low} sorting in PiPSC-derived neural cell populations compared to the unsorted neural cell population (Figure 4C). Percentages of NCAM-positive and β-tubulinIII-positive cells increased from >40% (before sorting) to >80 % after NCAM^{+}/CD29^{low} sorting. Percentages of TH, TH/FOXA2, and TH/EN1-positive cells increased significantly from >10 % (before sorting) to >35–40 % after sorting ($p< 0.01$, Figure 4C). In unsorted PiPSC-derived neural cell populations we detected transthyretin positive choroid plexus endothelium-type cells (<0.03% of total cell population). According to our results NCAM^{+}/CD29^{low} sorting eliminated transthyretin-positive cells from the DA neuron cell population, whereas after NCAM^{-} selection a few transthyretin-positive cells were detected (Figure 4F).

In vivo survival and functionality of unsorted and NCAM^{+}/CD29^{low} -sorted PiPSC-DA neurons in a Parkinsonian model rat

Characterization of PiPSC-derived DA neurons in vivo—Sixteen weeks after transplantation of unsorted PiPSC-derived DA neurons (from the MF95.06 line) formation of choroid plexus endothelium cell-type overgrowth was detected in the 6-OHDA rat

striatum (Figure 5A). The expression of the choroid plexus endothelium specific marker transthyretin was colocalized with human nuclear marker to confirm that cells originated from transplanted PiPSCs. Although, transthyretin expression was also detected in a few single cells in the PiPSC-line MF25.04-derived neural cell population *in vivo* and *in vitro* (< 0.03% from total cell population, Figure 4F), we did not detect any abnormal cell growth 16 weeks after transplantation of these cells (n=6, Figure 5A). The sorted $NCAM^{+}/CD29^{low}$ cell grafts were negative for transthyretin (PiPSC-line MF25.04). Sixteen weeks after transplantation, the presence of A9-type DA neurons was confirmed with FOXA2/TH/NCAM and FOXA2/TH/Girk2 staining both in unsorted and $NCAM^{+}/CD29^{low}$ PiPSC-derived DA-neuron grafts (Figure 5C and D). Rare FOXA2/TH/Calbindin positive A10-type DA neurons were detected both in unsorted and sorted neural grafts (Figure 5C and D). The DA neuron innervation to host striatum was visualized with TH/hNCAM staining (Figure 5E and F). To confirm the graft origin of innervating DA neurons in host tissue, co-localization of human NCAM was detected in TH-positive neurites (Figure 5G).

PiPSC-derived TH-positive DA neuron integration in host striatum and behavioral improvement of Parkinsonian rat model

The sorted PiPSC-derived neural grafts were smaller in size compared to unsorted cell grafts (Supplemental Figure 2, Figure 6A–B). However, the density of TH+ cells was significantly higher in the sorted $NCAM^{+}/CD29^{low}$-neural grafts compared to unsorted grafts (12,359±2015 TH+ cells/mm^3 unsorted grafts vs 28,621±6340 TH+ cells/mm^3 sorted grafts, $p<0.05$). The total number of TH+ DA neurons in the sorted $NCAM^{+}/CD29^{low}$ cell grafts in 6-OHDA rats striatum varied between 2,791–18,684 TH+ cells/graft (n=6). Two rats that were transplanted with sorted cells had only a few surviving cells 16 weeks after transplantation, these animals did not show behavioral recovery as expected [20] and they were excluded from the analysis. In the unsorted PiPSC-derived neural grafts. the number of TH+ DA neurons varied between 4,835–22,666 TH+ cells/graft (n=5). According to TH-DAB staining and ImageJ analysis, the TH-intensity in the lesioned striatum increased significantly in animals with unsorted or sorted neural cell grafts compared to lesioned controls without graft ($p< 0.05$, Supplemental Figure 3). Consistent with a previous study [20] and according to our histological analysis, 6-OHDA lesioned rats that had PiPSC-derived neural cell grafts with a sufficient number of surviving TH-positive neurons and TH + neurite outgrowth showed behavioral recovery. These animals had cell grafts with TH+ fiber outgrowth >31,000 TH+ fibers/mm^3 into the host striatum and they improved significantly on their rotational asymmetry in amphetamine-induced rotation-tests compared to lesioned-control animals (n=4, Figure 6). The transplanted $NCAM^{+}/CD29^{low}$ –animal group ($p<0.05$) and the unsorted PiPSC-neural group significantly increased their contralateral paw usage in the cylinder test compared to lesioned control animals (n=4, Figure 6).

Survival of non-human primate iPSC-derived DA neurons after autologous transplantation

Parkinsonian motor scores (PRS) were evaluated monthly, and were not altered at 12 months post-transplantation of PiPSC-derived neurons compared to the pre-transplantation score (pre-transplantation PRS = 11, PRS at 12 months post-transplantation = 10). Daytime activity measurements, determined using a global activity monitor were also not changed by transplantation (pre-transplantation activity= 27.69, post-transplantation activity = 34.39). One year after autologous transplantation, PiPSC-derived DA neurons survived in the monkey putamen and expressed FOXA2/TH/β-tubulinIII (Figure 7A). TH+ fiber outgrowth was also detected from the graft site (Figure 7A). Higher magnification showed co-localization of FOXA2/TH in the transplanted DA neurons (Figure 7B). TH-staining showed that the PiPSC-derived neural graft was located in putamen, and TH+ DA neurons were scattered throughout the graft (Figure 7C). In addition to DA neurons, some lipofuscin

granules were detected at the graft site (Figure 7C inset). Importantly, the PiPSC-derived neural cell graft did not contain any transthyretin positive cells and no graft overgrowth or cyst formation were detected in the monkey striatum 1 year after transplantation. To analyze immunoreactions in the host brain tissue and graft site we analyzed the histocompatibility (HLA) complex class II (MHC class II) positive cells with HLA-DAB staining. We observed a localized increase in microglial cell density around the needle tract, and labeling for MHC II showed cells with a macrophage morphology engorged with lipofuscin granules. Figure 7D shows the graft-host boundary with typical resting microglia around the graft; no glial scar formation was detected. According to in vitro characterization prior to transplantation, PiPSC-derived DA neurons (MF27.04-line) were positive for NCAM (>70%), β-tubulinIII (>20%), FOXA2 (>60%), TH (>10%), FOXA2/TH/β-tubulinIII (>3%), and CD29 (>40%). Transplanted cells were negative for the pluripotency markers Tra 1–81 and Tra 1–60 (Figure 7E–F). PiPSC-derived DA neurons were transplanted in the striatum of 6-OHDA-lesioned rats in parallel with the monkey transplantation. *In vivo* PiPSC-derived neurons expressed A9-type DA neuron markers FOXA2/TH/NCAM and FOXA2/TH/Girk2. Importantly, transplanted cells were negative for transthyretin (Supplemental Figure 4A–C). Four months after transplantation, grafted cells improved amphetamine-induced rotational asymmetry of 6-OHDA-lesioned rats compared to lesioned control animals without cell graft ($p < 0.05$, Supplemental Figure 4D).

Discussion

Currently there are no curative treatments for PD and existing drugs cause severe side effects diminishing the quality of patient lives. Stem cell-derived neural cell therapies are one option for replacing dead or dying VM DA neurons in the striatum of PD patients. In addition to clinically tested fetal cell transplants [1, 2] pluripotent stem cells, due to their efficient differentiation capacity, are considered to be ideal for neural differentiation and cell therapy for PD in the future [3–5]. Several research groups have developed differentiation methods for production of hESCs- or human iPSCs derived midbrain-type DA neurons [3–5]. Nonetheless, several key questions still remain to be solved in order to further improve these protocols for cell therapies. The aim of our study was to optimize the hESC-, hiPSC- and PiPSC-derived DA neuron differentiation protocol with a sorting step to achieve a safe and easily convertible method for clinical use in the future.

Differentiation of VM DA neurons from human embryonic stem cells

According to the data presented here, our adaptation of previous protocols results in high efficiency of hESC-DA neuron differentiation [3–5]. VM DA neuron differentiation of hESCs requires floor-plate induction with highly activated SHH (C24II or C25II) [21, 30]. Here we showed that after replacement of mouse/human recombinant SHH with the small molecule SAG (1 μM), which is a chlorobenzothiophene-containing Hh pathway agonist, the efficiency of DA neuron derivation from hESCs remained unchanged. We also showed that neural induction of hESCs in feeder-free cultures occurred with dual SMAD-inhibition as previously described [4, 21]. Also, a combination of the small molecules SB431542 and LDN193189 with the recombinant protein noggin resulted in efficient neural differentiation. In addition, we showed that activation of the wnt-signaling pathway in the presence of GSK-3β inhibitor CHIR is essential for derivation of FOXA2/OTX2+ DA neuron precursor cells and differentiation of FOXA2/TH+ VM DA neurons. These results are in line with a former study, which shows that derivation of DA-neurons from pluripotent stem cells requires temporal inhibition of GSK-3β with CHIR [4]. It has also been suggested that the concentration of the GSK-3β inhibitor is important for efficient and specific patterning of floor-plate derived DA-neurons [3, 5]. Related to these questions, we were able to

demonstrate that 1 μM CHIR during the first 13 days of differentiation was sufficient for DA neuron differentiation.

Characterization of floor-plate derived neural subpopulations and sorting of human VM DA neurons

Characterization of differentiated neural cell subpopulations is important for defining the surface protein expression profile for specific cell types *in vitro* [14, 15]. This profiling is important for selecting markers for enrichment of DA neuron precursors, and for qualification of a panel of markers for detecting unsafe cells from differentiated cell populations. Here we were able to show that hESC and hiPSC- floor-plate derived neural cell populations contained subpopulations of $NCAM^{low}$, $CD29^{+}$, $NCAM^{+}$, and $NCAM^{+}/CD29^{low}$ cells. From these subpopulations, the $NCAM^{low}$ population contained cells that expressed KDR, a marker for mesodermal cells [31, 32]. Also, a low level of the pluripotency marker SSEA-4 was detected in the $NCAM^{low}$ subpopulation. The $NCAM^{+}$ population included neural stem cells/precursors that were positive for $CD184^{+}/CD133^{low}$ [15, 16], and neuronal cells that were $CD24^{+}/CD29^{low}$ [14]. Gene expression profiling of these subpopulations showed that $NCAM^{+}/CD29^{low}$ cells had significantly higher expression levels of DA neuron specific mRNAs; *NURR1*, *GIRK2*, *PITX3* and *TH*, compared to the unsorted neural cell populations, $NCAM^{low}$, or $CD29^{+}$ cell populations. We selected $NCAM^{+}/CD29^{low}$ sorting for enrichment of DA neurons derived from hESCs and hiPSCs. FOXA2 and EN1 are transcription factors specially expressed in VM floor plate-derived progenitors, which are important for derivation of VM DA neurons [5]. Here, we showed that after sorting with $NCAM^{+}/CD29^{low}$ the neural cell population had significantly higher amounts of FOXA2/TH+ and EN1/TH+ DA neurons compared to unsorted cell populations (10%-20% prior to sorting vs. 40% after $NCAM^{+}/CD29^{low}$ sorting). Human VM contains two types of specialized DA neurons; A9-type cells which are located in substantia nigra pars compacta and A10-type cells which are located in ventral tegmental area [33]. Calbindin is a calcium binding protein, which is expressed in the vast majority of A10-type TH neurons. $NCAM^{+}/CD29^{low}$ sorting significantly decreased the number of Calbindin and FOXA2/TH/Calbindin-positive cells in the hiPSC-derived neural population compared to unsorted neural cell populations. Previous studies have suggested that only nigral A9 neurons are able to reinnervate degenerated striatum after transplantation [34, 35]. Thus, our sorting strategy is feasible for elimination of A10-type calbindin-positive DA neurons and enrichment of A9-type DA neurons, which is important for optimal cell population production for PD motor symptom treatment.

Differentiation and sorting of non-human primate iPSC-derived VM DA neurons

In order to assess the suitability of this differentiation protocol also for other primate cell lines, we studied cynomolgus macaque fibroblast-derived iPSC-lines in parallel with hESC and hiPSC lines. According to our results, DA neuron differentiation efficiency of PiPSCs showed no statistical differences compared to hESC- and hiPSC-differentiation *in vitro*.

To study the differentiation capacity and cell survival *in vivo* we transplanted sorted and unsorted PiPSC-derived DA neurons to 6-OHDA rat striatum. One of the unsorted PiPSC-line derived cell populations resulted in formation of transthyretin-positive choroid plexus epithelial cell type overgrowth. Normally, transthyretin is secreted by the choroid plexus epithelium into the cerebral spinal fluid and it has been described as a marker for primary choroid plexus neoplasms [36].

Infrequently, we were able to detect few individual transthyretin-positive cells also in the three other unsorted cell lines studied *in vitro* (<0.03%). However, we could not detect any transthyretin-positive cell overgrowth with these cell lines *in vivo*. Compared to this, the

sorted cell populations did not contain any transthyretin-positive cells *in vitro* or *in vivo* and no overgrowth was detected in any of the transplanted animals. We believe that this differentiation tendency to transthyretin-positive cells is caused by line-dependent individual differences and that it is independent of the differentiation protocol used. In all the studied PiPSC-lines the expression of SSEA-4 varied between 5–30% after differentiation, depending of the cell line studied. As previously shown, there are line dependent differences in the propensity for PiPSC-lines differentiation towards DA neurons [20]. The different genetic origin of cell lines may affect for the propensity to differentiate efficiently towards neural lineages. Consistent with this, it has previously been shown that there are differences between pluripotent stem cell-lines capacity to differentiate into neural cells; hESC-derived neural cells [37], hiPSC-derived neural cells [26]. These differences might also reflect the propensity of the cell lines for teratoma-, cyst-, or transthyretin-positive endothelial cell overgrowth *in vivo*. Most importantly, these results underline the importance of purification of cell populations, derived from different individual pluripotent stem cell lines, prior to transplantation.

Safety and functionality of sorted non-human primate iPSC-derived DA neurons *in vivo*

As our and other groups' studies have shown, pluripotent stem cell-derived neural cells entail risks of tumor formation upon transplantation if the cell population contains undifferentiated cells or proliferative non-neural cells [11–13]. For further purification of stem cell–derived cell populations and for enrichment of DA neurons, different transgenic ESC-lines with GFP-tagged promoters have been produced [17, 18]. However, genetic manipulation generates safety risks like increasing the risk of chromosomal mutations and tumorigenecity of cells. That is why surface protein based sorting is considered to be more optimal for clinical applications [14, 15]. Here, we demonstrated that sorting of PiPSC-derived neural cell population with $NCAM^{+}/CD29^{low}$ selection enriched the FOXA2/TH and EN1/TH-positive DA-neurons *in vitro* compared to unsorted cell population from >10% prior to sorting to >35–50% after sorting. Importantly, sorting of PiPSC-derived DA neurons with $NCAM^{+}/CD29^{low}$ selection prior to transplantation eliminated non-neural tumorigenic cells from the grafts and significantly increased the number of TH+ cells in the cell grafts compared to unsorted cell populations. To assess the functionality and connectivity of engrafted sorted DA-neurons with host striatal neurons, we performed amphetamine-induced rotation tests and cylinder tests for 6-OHDA-lesioned rats. According to our data, 16 weeks after transplantation 6-OHDA-lesioned rats with surviving cell grafts showed improved amphetamine-induced rotational asymmetry. Previously, it has been reported that a ~5% increase in the dopamine terminals in the striatum can improve the rotational asymmetry of lesioned animals in the amphetamine-induced rotation test [20, 38]. Thus the relatively low number of transplanted DA neurons and small graft sizes observed in the current study are still sufficient for behavioral recovery. According to the non-drug induced spontaneous movement test, 6-OHDA-lesioned rats with surviving cell grafts had increased use of their left paw compared to the lesioned control group without cell grafts. These results are important for proof of concept that sorted and enriched VM DA neuron populations are viable, safe and functional *in vivo*, and improve the behavioral outcome of PD-model rats, as previously shown with unsorted VM DA neurons [4].

iPSC-derived VM-DA neurons for autologous cell therapy of PD

Based on our studies it is important to use different animal models for preclinical transplantation studies of stem cell-derived neural cell grafts [20, 39]. Related to our results, we propose that a standard operation protocol for future clinical cell preparations should include *in vivo* safety-testing in PD-animal models to show absence of transthyretin-positive cells or other tumorigenic cell types. In addition with rodent PD-models, we think that for more accurate and scalable cell preparation and pre-clinical safety-testing stem cell-derived

DA neurons should be transplanted in non-human primate models of PD. Long-term studies of transplanted pluripotent stem cell-derived neurons are possible in non-human primates (>3 years), but impossible in rodents. Previously, it has been described that after transplantation of hESC-derived neural cells to non-human primate brain, the cell grafts were rejected in two out of three animals studied [40]. In spite of the fact that animals received cyclosporine for immunosupression, this study showed activation of immunoresponses in the graft site including CD45-positive leukocytes, CD68-positive microglia/macrophages and detection of necrotic cells in the remaining graft [40]. Although, the brain is an immunopriviledged site, immunoresponses in primates are complex [41]. Improved immunosupression paradigms, in addition to conventionally used cyclosporine, may be necessary for pre-clinical testing of human stem cell-derived xenografts in monkeys [40]. Related to this, our group has previously derived isogenic MHC-matched non-human primate iPSC-lines from cynomolgus macaques in order to overcome the difficulties of finding optimal immunosupression for primates [20]. Here, we show that non-human primate iPSC-derived neural cells survive after 1 year of autologous transplantation in a cynomolgus macaque brain, without any immunosupression. This PiPSC-derived neural cell graft contained DA neurons positive for TH/FOXA2. We did not detect any transthyretin-positive cells or abnormal overgrowth of the graft in the monkey striatum after 1 year. These results are also encouraging for the future of human iPSC-derived cells in clinical use.

For the future development of cell transplantation therapies for neuroregenerative diseases, hiPSCs possess several advantages compared to hESCs. hiPSCs are derived without the use of human fertilized eggs or embryos, diminishing the ethical questions related to embryonic stem cell therapies. Furthermore, there is an almost unlimited cell supply to generate patient specific iPSC lines from skin biopsies, which offers the opportunity to produce autologous cell grafts without immuno rejections [35]. In spite of these advantages, there are also several hurdles related to the use of iPSC in regenerative medicine, including the cells' epigenetic memory [42], old mitochondria [43], and reprogramming technology [44, 45]. iPSC cells are traditionally made by insertion of oncogenic genes (c-myc) by use of retroviruses, which can lead to an incomplete reprogramming process and make cells tumorigenic upon reactivation of transgenes or result in incomplete repression of transcription factors [44, 45]. Insufficient reprogramming can also induce abnormal gene expression in some iPSC-derived cells and induce T-cell-dependent immune response in syngeneic recipients [46]. The use of mutagenesis and virus-free iPSCs or non-integrating sendai-viruses will help to overcome these obstacles and widen the use of these cells in clinical research [47–51]. However, prior to entering clinics with stem cell-derived DA neurons, cell populations must be characterized thoroughly both *in vitro* and *in vivo* in terms of: identity, proliferation and differentiation capacity, purity, sterility, safety, and efficacy. Hopefully, after accomplishing all these requirements it will be possible to treat Parkinson's disease with pluripotent stem cell-derived DA neurons.

Supplementary Material

Refer to Web version on PubMed Central for supplementary material.

Acknowledgments

We would like to thank Tana Brown, Sarah Izen, Eduardo Perez-Torres, Jonathan Beagan and Melissa Hayes for excellent technical help. This work was supported by the NIH U24 grant (1U24NS078338-01), the Harvard Stem Cell Institute Translational Neuroscience Fund, the Orchard Foundation, the Harold and Ronna Cooper family, the Consolidated Anti-Aging Foundation, and the Poul Hansen family (OI), National Center for Research Resources RR00168 and the Office of Research Infrastructure Programs OD011103 (RS).

References

1. Ma Y, Tang C, Chaly T, et al. Dopamine cell implantation in Parkinson's disease: long-term clinical and (18)F-FDOPA PET outcomes. Journal of nuclear medicine: official publication, Society of Nuclear Medicine. 2010; 51(1):7–15.
2. Politis M, Wu K, Loane C, et al. Serotonergic neurons mediate dyskinesia side effects in Parkinson's patients with neural transplants. Science translational medicine. 2010; 2(38):38ra46.
3. Kirkeby A, Grealish S, Wolf DA, et al. Generation of regionally specified neural progenitors and functional neurons from human embryonic stem cells under defined conditions. Cell reports. 2012; 1(6):703–714. [PubMed: 22813745]
4. Kriks S, Shim JW, Piao J, et al. Dopamine neurons derived from human ES cells efficiently engraft in animal models of Parkinson's disease. Nature. 2011; 480(7378):547–551. [PubMed: 22056989]
5. Xi J, Liu Y, Liu H, et al. Specification of midbrain dopamine neurons from primate pluripotent stem cells. Stem cells. 2012; 30(8):1655–1663. [PubMed: 22696177]
6. Ono Y, Nakatani T, Sakamoto Y, et al. Differences in neurogenic potential in floor plate cells along an anteroposterior location: midbrain dopaminergic neurons originate from mesencephalic floor plate cells. Development. 2007; 134(17):3213–3225. [PubMed: 17670789]
7. Hynes M, Porter JA, Chiang C, et al. Induction of midbrain dopaminergic neurons by Sonic hedgehog. Neuron. 1995; 15(1):35–44. [PubMed: 7619528]
8. Prakash N, Brodski C, Naserke T, et al. A Wnt1-regulated genetic network controls the identity and fate of midbrain-dopaminergic progenitors in vivo. Development. 2006; 133(1):89–98. [PubMed: 16339193]
9. Ye W, Shimamura K, Rubenstein JL, et al. FGF and Shh signals control dopaminergic and serotonergic cell fate in the anterior neural plate. Cell. 1998; 93(5):755–766. [PubMed: 9630220]
10. Cooper O, Hargus G, Deleidi M, et al. Differentiation of human ES and Parkinson's disease iPS cells into ventral midbrain dopaminergic neurons requires a high activity form of SHH, FGF8a and specific regionalization by retinoic acid. Molecular and cellular neurosciences. 2010; 45(3):258–266. [PubMed: 20603216]
11. Doi D, Morizane A, Kikuchi T, et al. Prolonged maturation culture favors a reduction in the tumorigenicity and the dopaminergic function of human ESC-derived neural cells in a primate model of Parkinson's disease. Stem cells. 2012; 30(5):935–945. [PubMed: 22328536]
12. Sonntag KC, Pruszak J, Yoshizaki T, et al. Enhanced yield of neuroepithelial precursors and midbrain-like dopaminergic neurons from human embryonic stem cells using the bone morphogenic protein antagonist noggin. Stem cells. 2007; 25(2):411–418. [PubMed: 17038668]
13. Brederlau A, Correia AS, Anisimov SV, et al. Transplantation of human embryonic stem cell-derived cells to a rat model of Parkinson's disease: effect of in vitro differentiation on graft survival and teratoma formation. Stem cells. 2006; 24(6):1433–1440. [PubMed: 16556709]
14. Pruszak J, Ludwig W, Blak A, et al. CD15, CD24, and CD29 define a surface biomarker code for neural lineage differentiation of stem cells. Stem cells. 2009; 27(12):2928–2940. [PubMed: 19725119]
15. Sundberg M, Jansson L, Ketolainen J, et al. CD marker expression profiles of human embryonic stem cells and their neural derivatives, determined using flow-cytometric analysis, reveal a novel CD marker for exclusion of pluripotent stem cells. Stem cell research. 2009; 2(2):113–124. [PubMed: 19383417]
16. Yuan SH, Martin J, Elia J, et al. Cell-surface marker signatures for the isolation of neural stem cells, glia and neurons derived from human pluripotent stem cells. PloS one. 2011; 6(3):e17540. [PubMed: 21407814]
17. Ganat YM, Calder EL, Kriks S, et al. Identification of embryonic stem cell-derived midbrain dopaminergic neurons for engraftment. The Journal of clinical investigation. 2012; 122(8):2928–2939. [PubMed: 22751106]
18. Hedlund E, Pruszak J, Lardaro T, et al. Embryonic stem cell-derived Pitx3-enhanced green fluorescent protein midbrain dopamine neurons survive enrichment by fluorescence-activated cell sorting and function in an animal model of Parkinson's disease. Stem cells. 2008; 26(6):1526–1536. [PubMed: 18388307]

19. Cooper O, Seo H, Andrabi S, et al. Pharmacological rescue of mitochondrial deficits in iPSC-derived neural cells from patients with familial Parkinson's disease. Science translational medicine. 2012; 4(141):141ra190.
20. Deleidi M, Hargus G, Hallett P, et al. Development of histocompatible primate-induced pluripotent stem cells for neural transplantation. Stem cells. 2011; 29(7):1052–1063. [PubMed: 21608081]
21. Chambers SM, Fasano CA, Papapetrou EP, et al. Highly efficient neural conversion of human ES and iPS cells by dual inhibition of SMAD signaling. Nature biotechnology. 2009; 27(3):275–280.
22. Pruszak J, Sonntag KC, Aung MH, et al. Markers and methods for cell sorting of human embryonic stem cell-derived neural cell populations. Stem cells. 2007; 25(9):2257–2268. [PubMed: 17588935]
23. Ungerstedt U. 6-Hydroxy-dopamine induced degeneration of central monoamine neurons. Eur J Pharmacol. 1968; 5(1):107–110. [PubMed: 5718510]
24. Debeir T, Ginestet L, Francois C, et al. Effect of intrastriatal 6-OHDA lesion on dopaminergic innervation of the rat cortex and globus pallidus. Exp Neurol. 2005; 193(2):444–454. [PubMed: 15869947]
25. Deumens R, Blokland A, Prickaerts J. Modeling Parkinson's disease in rats: an evaluation of 6-OHDA lesions of the nigrostriatal pathway. Exp Neurol. 2002; 175(2):303–317. [PubMed: 12061862]
26. Hargus G, Cooper O, Deleidi M, et al. Differentiated Parkinson patient-derived induced pluripotent stem cells grow in the adult rodent brain and reduce motor asymmetry in Parkinsonian rats. Proceedings of the National Academy of Sciences of the United States of America. 2010; 107(36): 15921–15926. [PubMed: 20798034]
27. Astradsson A, Jenkins BG, Choi JK, et al. The blood-brain barrier is intact after levodopa-induced dyskinesias in parkinsonian primates--evidence from in vivo neuroimaging studies. Neurobiol Dis. 2009; 35(3):348–351. [PubMed: 19501164]
28. Sanchez-Pernaute R, Studer L, Ferrari D, et al. Long-term survival of dopamine neurons derived from parthenogenetic primate embryonic stem cells (cyno-1) after transplantation. Stem Cells. 2005; 23(7):914–922. [PubMed: 15941857]
29. Mann TM, Williams KE, Pearce PC, et al. A novel method for activity monitoring in small non-human primates. Lab Anim. 2005; 39(2):169–177. [PubMed: 15901360]
30. Fasano CA, Chambers SM, Lee G, et al. Efficient derivation of functional floor plate tissue from human embryonic stem cells. Cell stem cell. 2010; 6(4):336–347. [PubMed: 20362538]
31. Kataoka H, Takakura N, Nishikawa S, et al. Expressions of PDGF receptor alpha, c-Kit and Flk1 genes clustering in mouse chromosome 5 define distinct subsets of nascent mesodermal cells. Development, growth & differentiation. 1997; 39(6):729–740.
32. Fujiwara M, Yan P, Otsuji TG, et al. Induction and enhancement of cardiac cell differentiation from mouse and human induced pluripotent stem cells with cyclosporin-A. PloS one. 2011; 6(2):e16734. [PubMed: 21364991]
33. Mendez I, Sanchez-Pernaute R, Cooper O, et al. Cell type analysis of functional fetal dopamine cell suspension transplants in the striatum and substantia nigra of patients with Parkinson's disease. Brain: a journal of neurology. 2005; 128(Pt 7):1498–1510. [PubMed: 15872020]
34. Schultzberg M, Dunnett SB, Bjorklund A, et al. Dopamine and cholecystokinin immunoreactive neurons in mesencephalic grafts reinnervating the neostriatum: evidence for selective growth regulation. Neuroscience. 1984; 12(1):17–32. [PubMed: 6146944]
35. Thompson L, Barraud P, Andersson E, et al. Identification of dopaminergic neurons of nigral and ventral tegmental area subtypes in grafts of fetal ventral mesencephalon based on cell morphology, protein expression, and efferent projections. The Journal of neuroscience: the official journal of the Society for Neuroscience. 2005; 25(27):6467–6477. [PubMed: 16000637]
36. Herbert J, Cavallaro T, Dwork AJ. A marker for primary choroid plexus neoplasms. The American journal of pathology. 1990; 136(6):1317–1325. [PubMed: 2356863]
37. Lappalainen RS, Salomaki M, Yla-Outinen L, et al. Similarly derived and cultured hESC lines show variation in their developmental potential towards neuronal cells in long-term culture. Regenerative medicine. 2010; 5(5):749–762. [PubMed: 20868330]

38. Bjorklund LM, Sanchez-Pernaute R, Chung S, et al. Embryonic stem cells develop into functional dopaminergic neurons after transplantation in a Parkinson rat model. Proc Natl Acad Sci U S A. 2002; 99(4):2344–2349. [PubMed: 11782534]
39. Sundberg M, Andersson PH, Akesson E, et al. Markers of pluripotency and differentiation in human neural precursor cells derived from embryonic stem cells and CNS tissue. Cell transplantation. 2011; 20(2):177–191. [PubMed: 20875224]
40. Emborg ME, Zhang Z, Joers V, et al. Intracerebral Transplantation of Differentiated Human Embryonic Stem Cells to Hemiparkinsonian Monkeys. Cell transplantation. 2012
41. Cicchetti F, Fodor W, Deacon TW, et al. Immune parameters relevant to neural xenograft survival in the primate brain. Xenotransplantation. 2003; 10(1):41–49. [PubMed: 12535224]
42. Kim K, Doi A, Wen B, et al. Epigenetic memory in induced pluripotent stem cells. Nature. 2010; 467(7313):285–290. [PubMed: 20644535]
43. Parker GC, Acsadi G, Brenner CA. Mitochondria: determinants of stem cell fate? Stem cells and development. 2009; 18(6):803–806. [PubMed: 19563264]
44. Okita K, Ichisaka T, Yamanaka S. Generation of germline-competent induced pluripotent stem cells. Nature. 2007; 448(7151):313–317. [PubMed: 17554338]
45. Ahrlund-Richter L, De Luca M, Marshak DR, et al. Isolation and production of cells suitable for human therapy: challenges ahead. Cell stem cell. 2009; 4(1):20–26. [PubMed: 19058776]
46. Zhao T, Zhang ZN, Rong Z, et al. Immunogenicity of induced pluripotent stem cells. Nature. 2011; 474(7350):212–215. [PubMed: 21572395]
47. Kaji K, Norrby K, Paca A, et al. Virus-free induction of pluripotency and subsequent excision of reprogramming factors. Nature. 2009; 458(7239):771–775. [PubMed: 19252477]
48. Woltjen K, Michael IP, Mohseni P, et al. piggyBac transposition reprograms fibroblasts to induced pluripotent stem cells. Nature. 2009; 458(7239):766–770. [PubMed: 19252478]
49. Soldner F, Hockemeyer D, Beard C, et al. Parkinson's disease patient-derived induced pluripotent stem cells free of viral reprogramming factors. Cell. 2009; 136(5):964–977. [PubMed: 19269371]
50. Yu J, Hu K, Smuga-Otto K, et al. Human induced pluripotent stem cells free of vector and transgene sequences. Science. 2009; 324(5928):797–801. [PubMed: 19325077]
51. Zhou H, Wu S, Joo JY, et al. Generation of induced pluripotent stem cells using recombinant proteins. Cell stem cell. 2009; 4(5):381–384. [PubMed: 19398399]

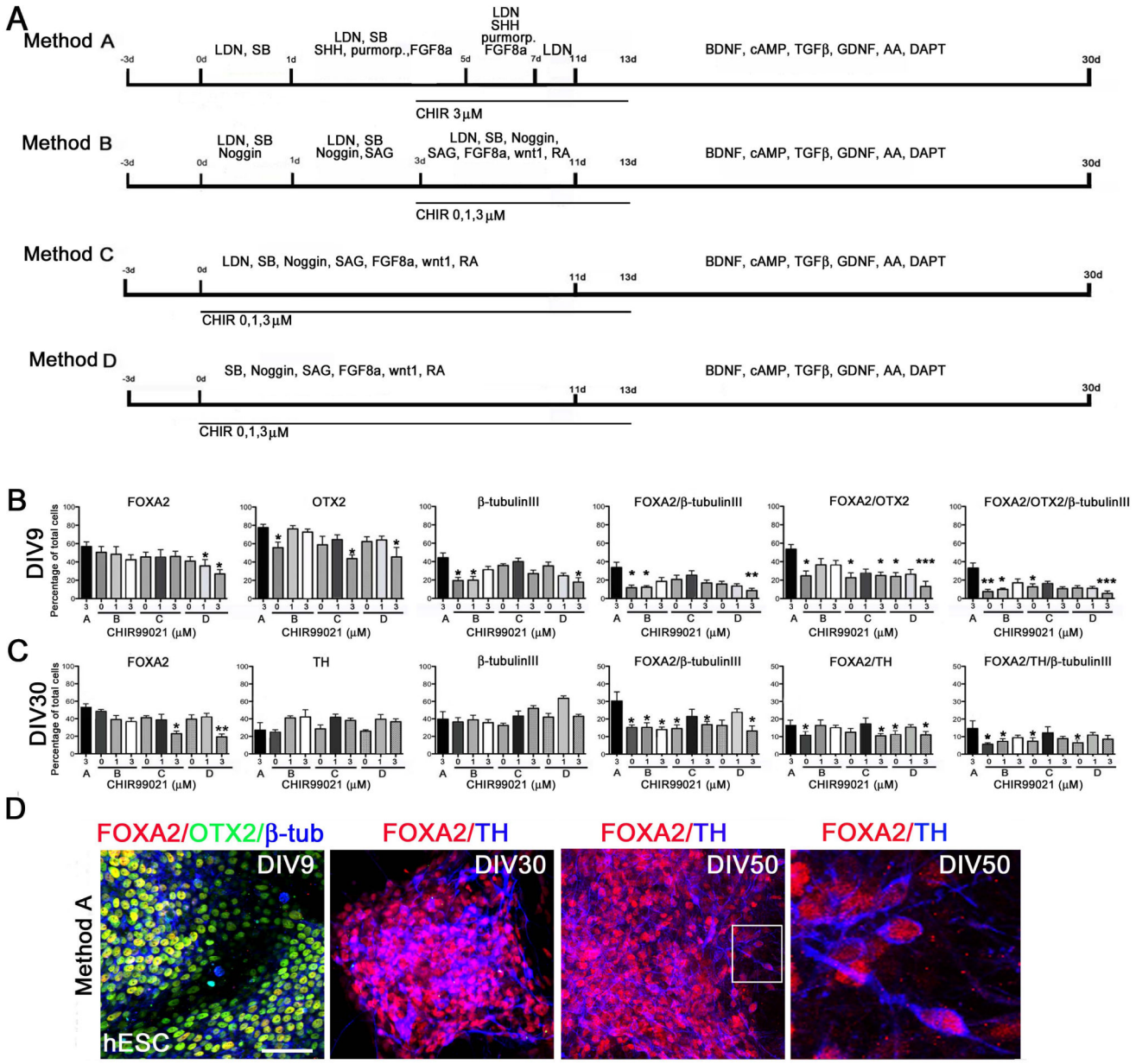

Figure 1. Differentiation of hESCs to DA neurons using small molecules

Panel A. Schematic presentation of the conditions tested for human DA neuron differentiation. Method A) LDN, SB, SHH (C24-II), purmorphamine, FGF8a and CHIR (3μM) were used for DA neuron derivation. Method B) cells were differentiated with sequential addition of LDN, SB, noggin, SAG, wnt1, FGF8a, RA, +/−CHIR (0, 1, 3 μM). Method C) cells were differentiated by simultaneous addition of LDN, SB, noggin, SAG, wnt1, FGF8a, RA, +/−CHIR (0, 1, 3 μM). Method D) cells were differentiated by simultaneous addition of noggin, SB, SAG, wnt1, FGF8a, RA, +/−CHIR (0, 1, 3 μM). **Panel B.** Immunocytochemical characterization of hESC-derived neural precursor cells. Number of FOXA2, OTX2, β-tubulinIII, FOXA2/β-tubulinIII, FOXA2/OTX2, and FOXA2/OTX2/β-tubulinIII-positive cells were analyzed after 9 days in vitro (DIV9). **Panel C.** Immunocytochemical characterization of hESC-derived DA neurons. Number of FOXA2, TH, β-tubulinIII, FOXA2/β-tubulinIII, FOXA2/TH, and FOXA2/TH/β-tubulinIII-positive

cells were analyzed after 30 days in vitro (DIV30). Statistical analysis was done with Kruskall-Wallis test (non-parametric ANOVA) and Dunn's multiple comparison test between selected pairs, significant differences between Method A and other conditions are presented * $p<0.05$, ** $p<0.01$, *** $p< 0.001$. **Panel D.** Representative images of hESC-derived ventral midbrain type neural precursors positive for FOXA2/OTX2/β-tubulinIII (DIV9) and DA neurons positive for FOXA2/TH (DIV30 and DIV50). Scale bar 50 μm.

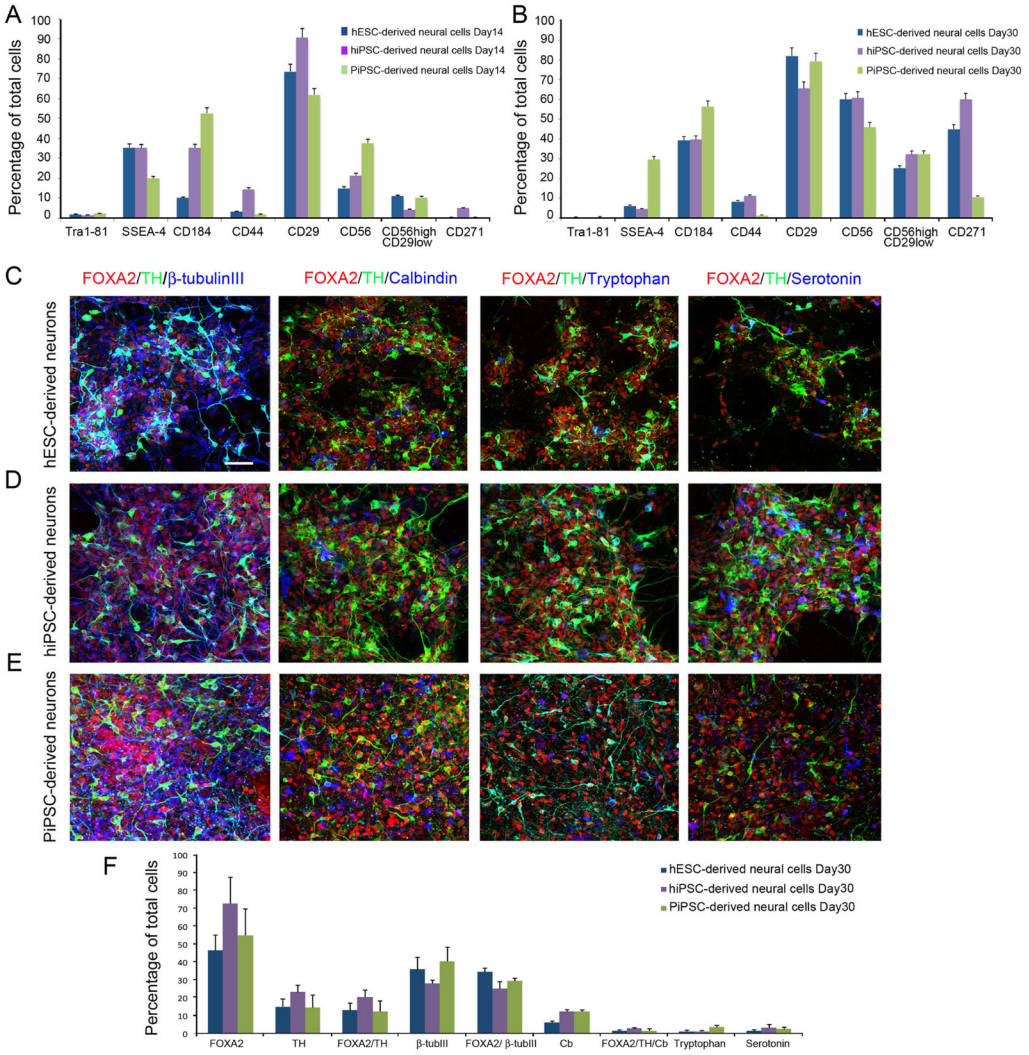

Figure 2. Characterization of hESC-, hiPSC- and PiPSC- derived DA neurons

A. Surface protein expression profile for hESC-, hiPSC-, and PiPSC-derived DA neuron precursors at day 14, and **B.** at day 30. Cells were differentiated according to Method A. **C–E.** After 30 days of in vitro differentiation (DIV30) hESC- **(C)**, hiPSC- **(D)** and PiPSCs-derived **(E)** DA-neurons express: FOXA2/TH/β-tubulinIII, FOXA2/TH/Calbindin, FOXA2/TH/Tryptophan hydroxylase, and FOXA2/TH/serotonin. **F.** Percentages of FOXA2, TH, FOXA2/TH, β-tubulinIII, FOXA2/β-tubulinIII, Calbindin, FOXA2/Calbindin, FOXA2/TH/Calbindin, Tryptophan hydroxylase/TH-negative, and Serotonin/TH-negative cells were analyzed, DIV30. Scale bar 50 μm.

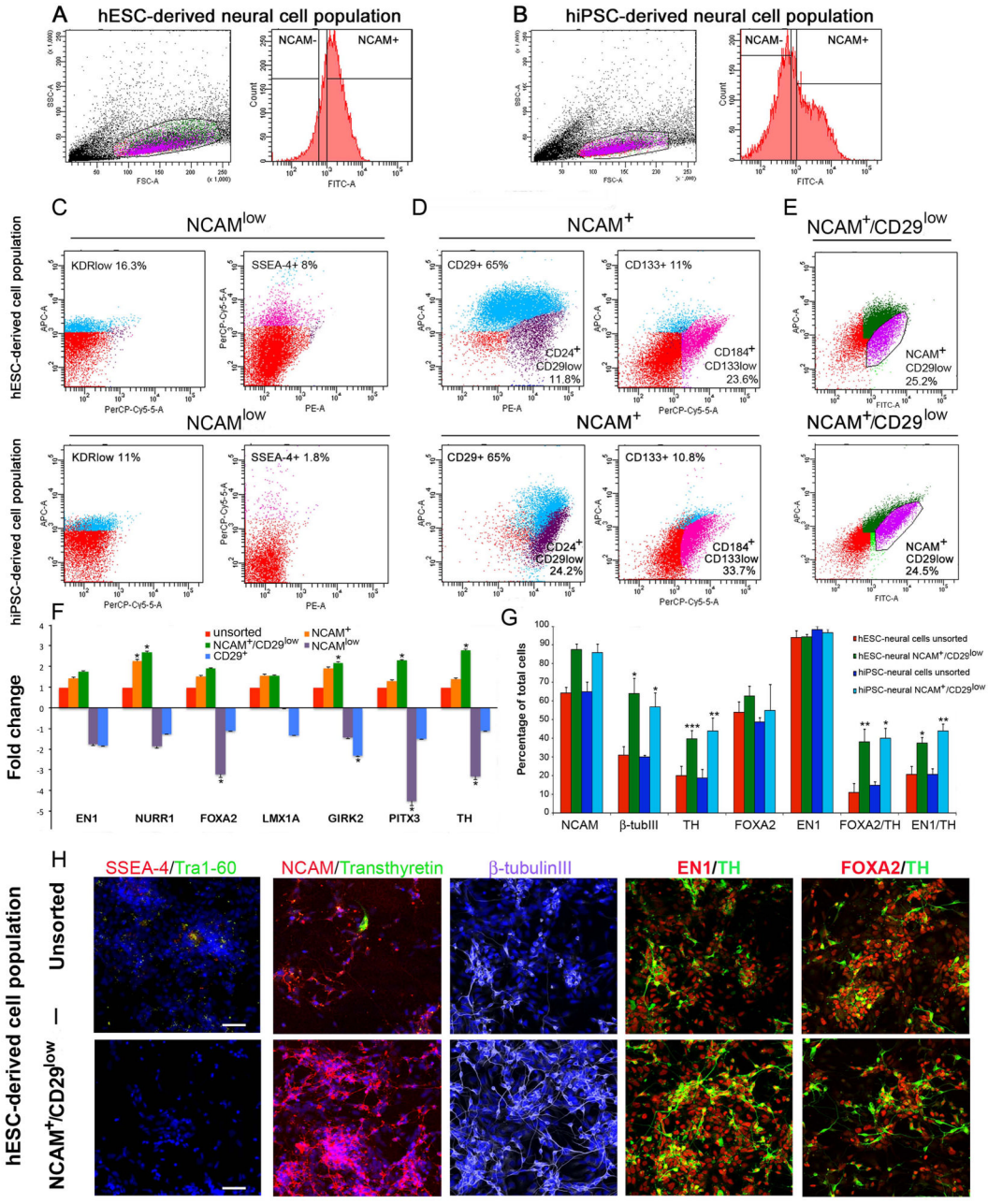

Figure 3. Enrichment of hESC- and hiPSC-derived DA neurons with cell sorting

Population determination and gating strategy for **A.** hESC-derived neural cell population and **B.** hiPSC-derived neural cell population with NCAM-staining. Characterization of subpopulations derived from hESC- and hiPSC-neural cell populations: **Panel C.** NCAM^{low} subpopulation was positive for KDR^{low} (11–16.3%) and SSEA-4 (1.8–8%). **Panel D.** NCAM^{+} subpopulation was positive for CD29 (65%), CD133 (10.8–11%), CD184^{+}/CD133^{low} (23.6–33.7%). **Panel E.** Out of the total cell population, the NCAM^{+}/CD29^{low} subpopulation was 24.5–25.2%. **F.** Q-RT-PCR analysis shows that the NCAM^{+}/CD29^{low} subpopulation has an upregulated DA neuron specific gene expression profile compared to the unsorted cell population and the NCAM^{+}, NCAM$^{−}$, and CD29^{+} subpopulations. **G.** Immunocytochemical cell counts reveal that hESC- and hiPSC-derived NCAM^{+}/CD29^{low}

sorted cell populations have enriched expression of NCAM, β-tubulinIII, TH, FOXA2/TH, EN1/TH cells compared to unsorted cell populations. **Panel H.** Immunocytochemical characterization of the unsorted hESC-derived DA neuron population. **Panel I.** Immunocytochemical analysis of the $NCAM^{+}/CD29^{low}$ sorted hESC-derived DA neuron population. Scale bar 50 μm.

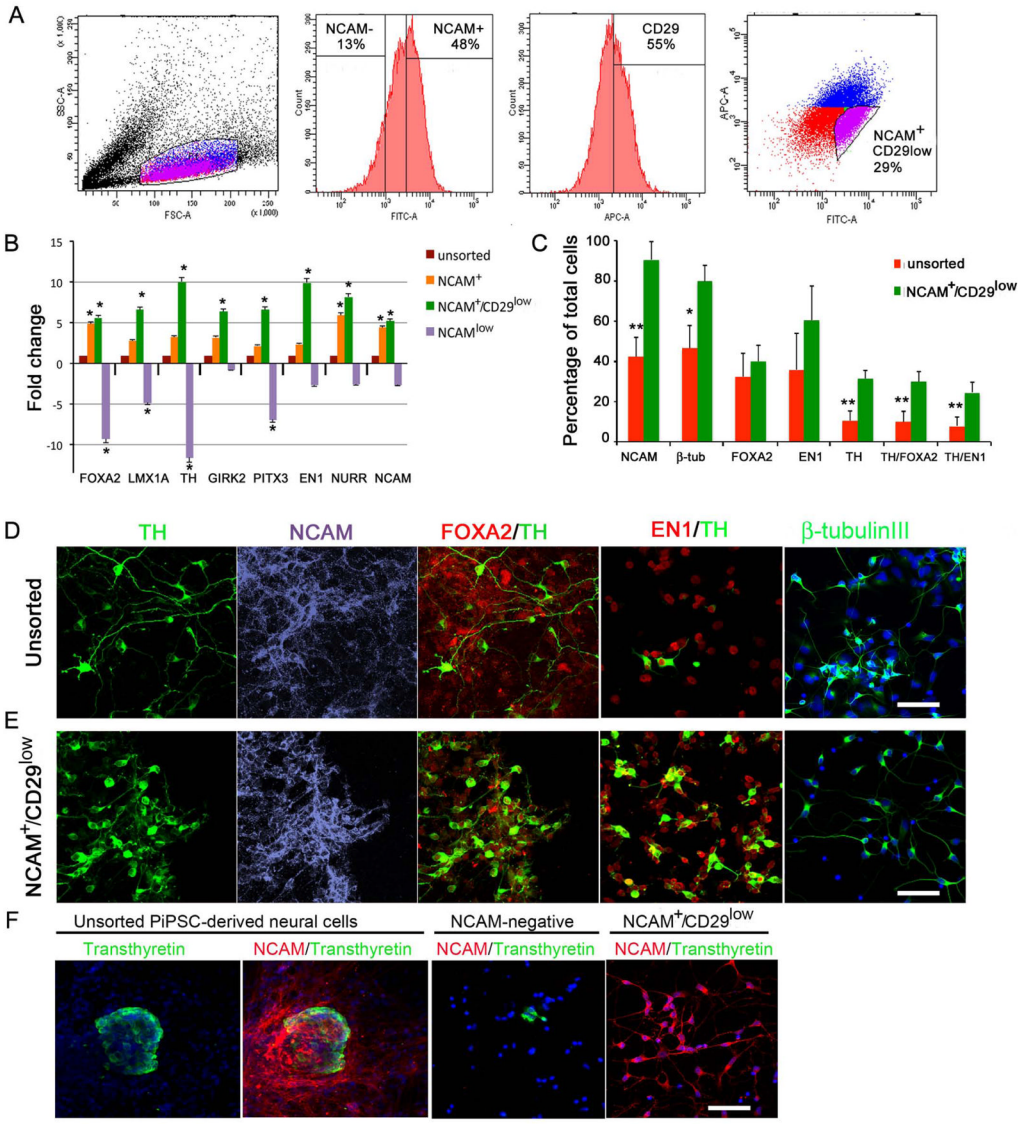

Figure 4. Enrichment of PiPSC-derived DA neurons with cell sorting

Panel A. Population determination and gating strategy for cell sorting according to SSC/FSC dot plot. Histograms show percentages of NCAM−/+ cells, and CD29+ cells. FITC/APC dot plot shows gating strategy for sorting of NCAM^{+}/CD29^{low} cells according to fluorescence intensity. **B.** Gene expression analysis with DA-neuron specific markers: *FOXA2, LMX1A, TH, GIRK2, PITX3, EN1, NURR1, NCAM.* Relative fold change in gene expression of sorted NCAM-, NCAM+ and NCAM+CD29low cells was compared to unsorted cells (=1). **C.** Percentages of NCAM, β-tubulinIII, FOXA2, EN1, TH, TH/FOXA2, TH/EN1 positive cells in unsorted cell population, NCAM+ and NCAM^{+}/CD29^{low} cell population. Statistical analysis was performed with Kruskall-Wallis test (non-parametric ANOVA) and Dunn's multiple comparison test between selected pairs. Significant differences between unsorted and sorted NCAM+CD29low cells are presented * $p<0.01$, ** $p< 0.001$. **Panels D–E.** Immunocytochemical characterization of unsorted **(D)** and sorted NCAM^{+}/CD29^{low} cells **(E)** with TH, NCAM, FOXA2/TH, EN1/TH and β-tubulinIII staining. **Panel F.** Unsorted PiPSC-derived neural cells express transthyretin in small cell

clusters, and a few transthyretin-positive cells were detected after NCAM-negative sorting. $NCAM^{+}/CD29^{low}$ cells were negative for transthyretin. Scale bar 50 μm.

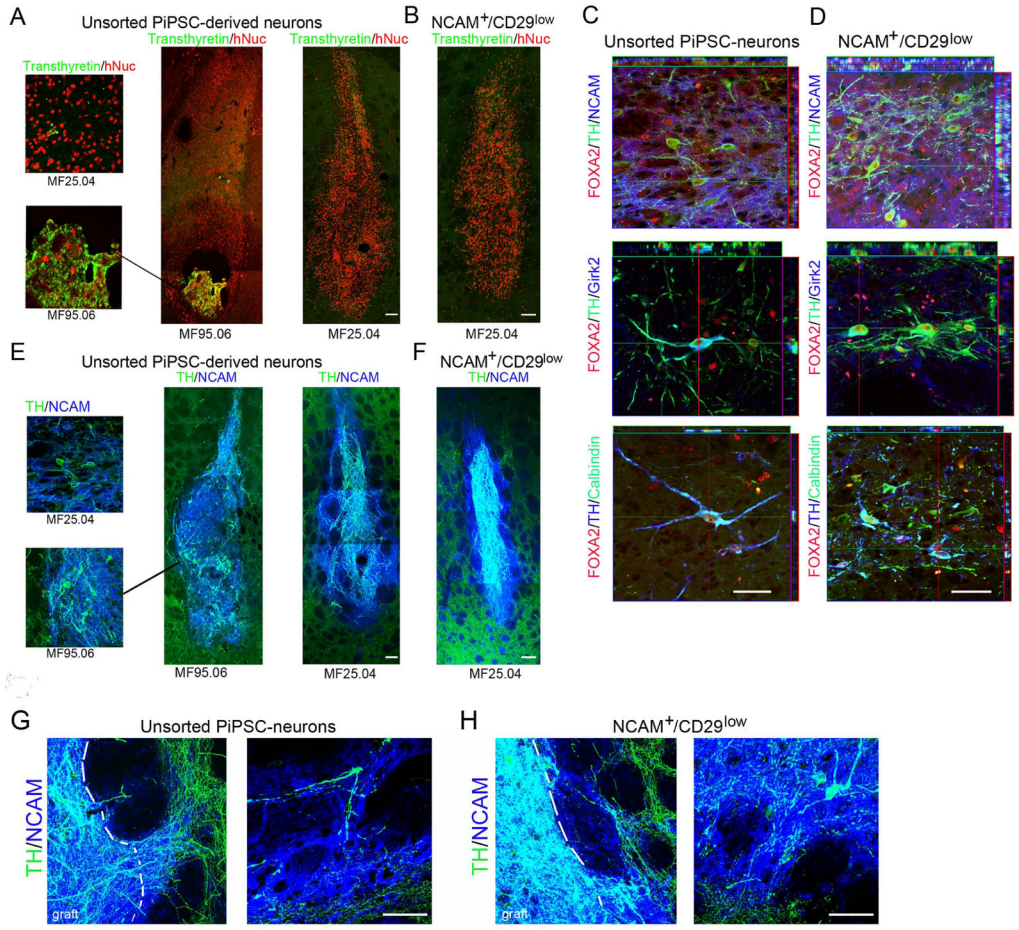

Figure 5. ***In vivo*** **characterization of unsorted and NCAM^{+}/CD29^{low} -sorted PiPSC-derived DA neurons in Parkinsonian model rat**

A. Unsorted PiPSC-derived neural grafts include overgrowth of tranthyretin- positive cells (MF95.06-line). No overgrowth was detected in other PiPSC-lines studied, although a few individual transthyretin-positive cells were present in the unsorted PiPSC-derived neural cell graft (MF25.04-line). **B.** NCAM^{+}/CD29^{low} sorted PiPSC-derived neural graft did not contain any tranthyretin–positive cells, scale bar 100 μm. **C.** Unsorted and **D.** Sorted PiPSC-derived DA-neuron cell grafts included FOXA2/TH/NCAM, FOXA2/TH/Girk2, and a few FOXA2/TH/Calbindin positive cells, scale bar 50 μm. **E.** Unsorted and **F.** NCAM^{+}/CD29^{low} sorted PiPSC-derived neural cell grafts were positive for TH/NCAM, scale bar 100 μm. **G–H.** Higher magnification of unsorted and sorted PiPSC-derived neural grafts shows graft derived TH/NCAM+ neurite innervation to host striatum. Co-localization of human NCAM marker with TH-positive neurites confirms graft origin of innervating neurites, scale bar 50 μm.

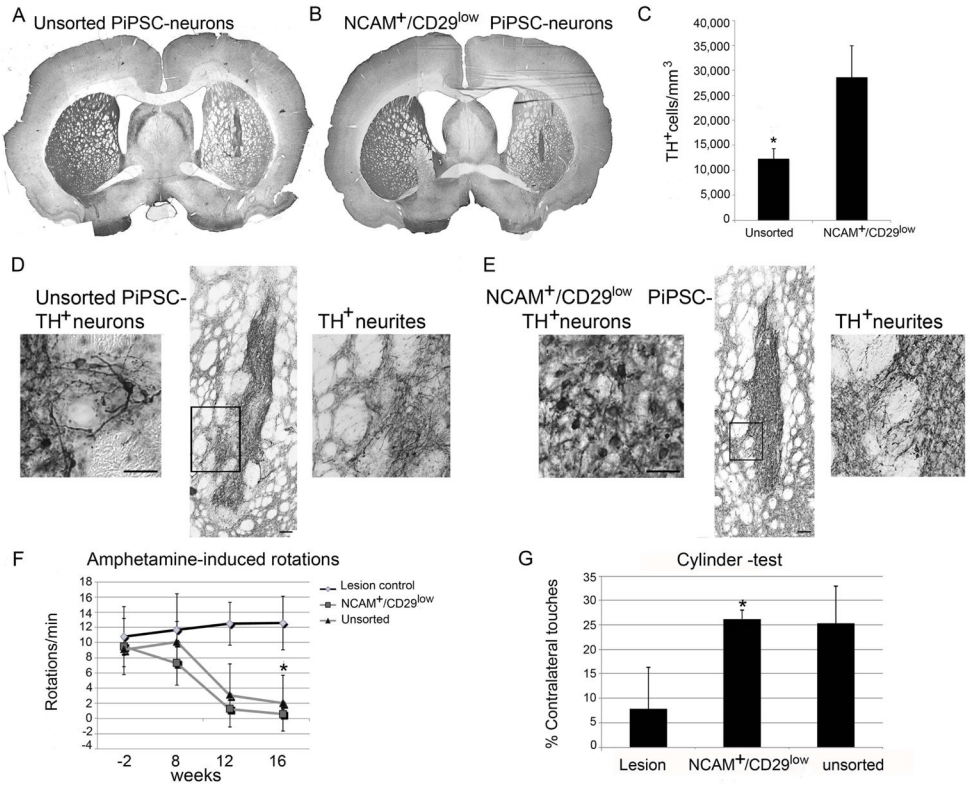

Figure 6. ***In vivo*** **survival of TH+ DA neurons and behavioral analysis of 6-OHDA rats transplanted with PiPSC-derived DA neurons**

A. Unsorted PiPSC-derived DA neuron graft express TH. **B.** Sorted NCAM^{+}/CD29^{low} PiPSC-derived DA neuron graft express TH. **C.** TH+ cell density is significantly higher in sorted NCAM^{+}/CD29^{low} cell graft compared to unsorted cell graft, * $p<0.05$. **D–E.** Higher magnification of unsorted cells and sorted NCAM^{+}/CD29^{low} -cells in the graft, scale bar 50 μm. Unsorted and NCAM^{+}/CD29^{low} cell grafts have TH+ neurite outgrowth from the graft site to the rodent host striatum, scale bar 100 μm. Higher magnification shows single TH+ neurites innervation to host striatum (black gate). **F.** Amphetamine-induced rotation tests for 6-OHDA-lesioned rats 8, 12, and 16 weeks after PiPSC-derived DA-neuron transplantations, show a graft-induced decrease in the number of rotations. **G.** Cylinder test in 6-OHDA rats at 16 weeks after transplantation of unsorted or sorted PiPSC-derived DA neurons. Rats with sorted NCAM^{+}/CD29^{low} neural grafts had significantly increased use of contralateral paw, * $p< 0.05$.

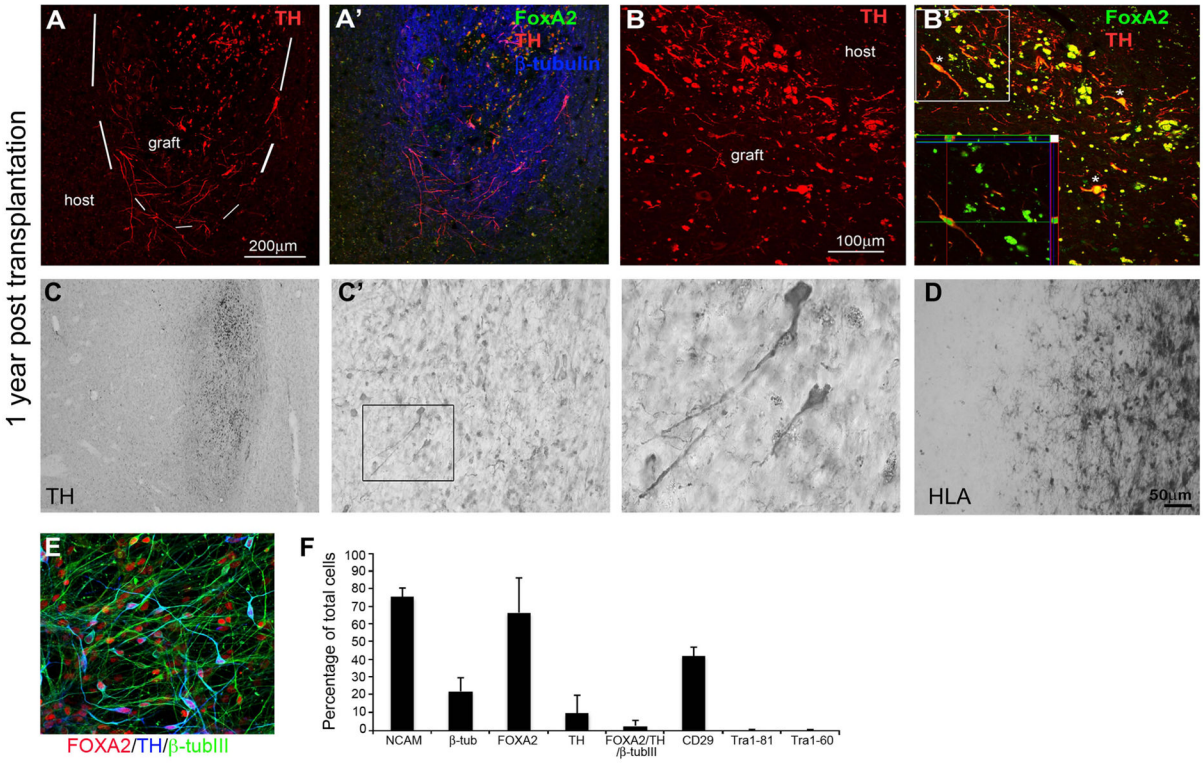

Figure 7. PiPSC-derived DA neuron graft survival in monkey striatum 1 year after autologous transplantation

A. TH+ DA neurons in the PiPSC-derived neural cell graft in cynomolgus macaque left putamen (MF27.04). **A′** FOXA2/TH/β-tubulinIII positive neural cells in the graft. **B.** The graft contained DA neurons that were double labelled for TH/FOXA2 **(B′). C**. TH-staining shows localization of PiPSC-derived neural graft in left putamen. **C′** Higher magnification shows scattering of TH+ DA neurons around the graft and some lipofuscin cells in the graft (inset). **D.** HLA-staining in the graft-host boundary (the host putamen is on the left of the image, graft on the right) shows typical resting microglia around the graft and no glial scar. **E.** *In vitro* characterization of PiPSC-derived DA neurons prior transplantation (MF27.04-line) shows that cells were positive for FOXA2/TH/β-tubulinIII. **F.** Percentages of NCAM, β-tubulinIII, FOXA2, TH, FOXA2/TH/β-tubulinIII, CD29, Tra 1–81, and Tra 1–60 in the cell population prior to transplantation.